

PP spherical-wave reflection coefficients for viscoelastic media

Vlastislav Červený ¹⁾, Ivan Pšenčík ²⁾ and Václav Bucha ¹⁾

¹⁾ Charles University in Prague, Faculty of Mathematics and Physics, Department of Geophysics, Ke Karlovu 3, 121 16 Praha 2, Czech Republic. E-mail: vcerveny@seis.karlov.mff.cuni.cz; bucha@seis.karlov.mff.cuni.cz

²⁾ Institute of Geophysics, Acad. Sci. of Czech Republic, Boční II, 141 31 Praha 4, Czech Republic. E-mail: ip@ig.cas.cz

Summary

Amplitudes of PP spherical waves reflected at a plane interface between two homogeneous viscoelastic media are studied. Mostly, the plane-wave reflection coefficients have been used in such studies in the past. For viscoelastic media, however, the meaning of plane-wave reflection coefficients meets some fundamental difficulties. For this reason, the spherical-wave reflection coefficients, corresponding to a point source, are used here. The spherical-wave reflection coefficients were introduced for perfectly elastic media and were evaluated by approximate asymptotic high-frequency methods. They can be, however, also calculated by highly accurate reflectivity method, even for viscoelastic media. The typical feature of the amplitude of the spherical-wave reflection coefficient is its behaviour in the critical region, which differs significantly from the behaviour of the amplitude of the plane-wave reflection coefficient. Its maximum is shifted behind the critical point, and it is followed by the amplitude oscillations in the interference region with the head wave. The position of the maximum, its magnitude and the oscillations are frequency-dependent. The purpose of this study is to show that the position of the maximum of the spherical-wave reflection coefficient depends only very weakly on the quality factors Q of media above and below the interface, and can thus hardly be used to determine Q from measurements. Another purpose is to find some other simple measurable quantities which depend on Q more strongly and would be thus more convenient for the solution of inverse problem for Q . It is shown that one of such quantities could be the difference between the maximum and following minimum of the amplitude of the spherical-wave reflection coefficient in the oscillatory zone behind the critical point.

Key words: spherical-wave reflection coefficients, critical region, viscoelastic media. reflectivity method

Seismic Waves in Complex 3-D Structures, Report 23, Charles University in Prague, Faculty of Mathematics and Physics, Department of Geophysics, Praha 2013, pp. 219–235

1 Introduction

In seismic exploration for oil, the amplitudes of reflected elastic waves have been broadly used to determine the velocities under the structural interfaces, at which the measured reflected waves are generated. The AVO (amplitudes-versus-offset) method has been broadly used for this purpose. For small offsets, i.e., for small angles of incidence i (the angle i is an acute angle, which slowness vector of the incident wave makes with the normal to the interface), it is usually sufficient to exploit plane-wave reflection coefficients to obtain acceptably accurate results. For larger offsets, however, the application of plane-wave reflection coefficients becomes very inaccurate, particularly if the velocity V_1 above the interface is smaller than the velocity V_2 beneath the interface and the difference between V_1 and V_2 is significant (strong contrast interface), see, e.g., Skopintseva et al. (2011). In this case, a very important role is played by the critical angle i^* , given by the relation

$$\sin i^* = V_1/V_2 . \quad (1)$$

1.1 Acoustic case

To simplify the explanations, we shall first consider acoustic waves in non-dissipative fluid media only. Only later, we shall discuss also the elastic and dissipative media. For acoustic pressure plane waves in fluid media, the plane-wave reflection coefficient is very simple. For normal incidence it equals $(z_2 - z_1)/(z_2 + z_1)$, where z is the wave impedance and equals $z = \rho V$, where ρ is the mass density. With increasing angle of incidence i , but still at subcritical region, the plane-wave reflection coefficient is real-valued. It first increases weakly with the angle of incidence. Close to the critical angle, however, it starts to increase rapidly and for the critical angle it reaches unity. The derivative of the plane-wave reflection coefficient with respect to the angle of incidence at the critical angle from the side of $i < i^*$ is infinite. For overcritical angles $i > i^*$, the plane-wave reflection coefficient is complex-valued, and equals $e^{i\varphi}$, where φ is the phase. Consequently, the amplitude of the pressure plane-wave reflections coefficient in the overcritical region is constant and equals unity. The phase of the plane-wave reflection coefficient in the overcritical region decreases from 0^0 at the critical angle to $-\pi$ for the angle of grazing incidence. Although the plane-wave reflection coefficient is complex-valued in the overcritical region, it is frequency independent.

For an incident spherical wave, generated by a point source situated in the medium of lower velocity, the situation is considerably different, particularly in the vicinity of the critical point. Formally, we can introduce the spherical-wave reflection coefficients. In contrast to the plane-wave reflection coefficients, they are frequency dependent and complex valued for all angles of incidence. In subcritical region, the frequency dependence is very weak, particularly for nearly normal incidence, but it is very strong in the critical region, where it completely changes the behaviour of the reflection coefficient when compared with the plane-wave reflection coefficient.

The spherical-wave reflection coefficient at a plane interface between two homogeneous non-dissipative fluid media (acoustic case) was first introduced and numerically studied

using the asymptotic high-frequency methods by Červený and Hron (1961). The asymptotic high-frequency procedures proposed by Brekhovskikh (1957) were used in that study. We do not present here the appropriate theory, we only emphasize that it is necessary to take into account the head wave, which is generated for overcritical angles of incidence. As mentioned, the spherical-wave reflection coefficients are frequency dependent. For $f \rightarrow \infty$, the plane-wave reflection coefficients are obtained. For finite frequencies, the differences between the spherical- and plane-wave reflection coefficients are very small in subcritical region. They become, however, significant in the critical region. The amplitudes of the spherical-wave reflection coefficients do not have singularity at the critical angle. They have their maximum behind the critical point. The distance between the maximum of the spherical-wave reflection coefficient and the critical point is frequency dependent. It increases with decreasing frequency. Behind the maximum, the amplitude of the reflection coefficient of a spherical wave oscillates. This oscillation of the coefficient with the distance is caused by the interference of the reflected and head waves. For this reason, we also speak of interference reflected-head wave.

In Figure 1, all the above properties of reflection coefficients of acoustic spherical harmonic waves are well demonstrated. The figure, which was calculated by asymptotic high-frequency methods, is taken from Červený and Hron (1961). The figure shows amplitudes (left column) and phases (right column) of the spherical-wave reflection coefficients. The spherical-wave reflection coefficients are displayed in bold. For comparison, also the reflection coefficients of plane waves are displayed, by thin dashed lines. The refractive index $n = V_1/V_2 = 0.4$ and the density ratio $\rho_1/\rho_2 = 1$ are considered. Individual plots in each column are specified by the dimensionless factor $k(z + z_0)$ related to the frequency f . Here k is the wave number, z is the distance of the receiver from the interface and z_0 is the distance of the source from the interface. Consequently, $k(z + z_0) = 2\pi(z + z_0)V_1^{-1}f$. The frequency thus decreases from the upper plots to the bottom plots. The whole range of angles of incidence i , from $i = 0^\circ$ to $i = 90^\circ$, is considered.

From Figure 1, we can clearly see that the plane-wave coefficients (with amplitudes A_0^* and phases φ_0^*) are frequency independent, but the spherical-wave reflection coefficients (with amplitudes A^* and phases φ^*) vary with frequency through the factor $k(z + z_0)$. Whereas the plane-wave reflection coefficients have discontinuous derivatives at the critical point, the spherical wave reflection coefficients are quite smooth there. The maximum of the amplitude-distance curve of A^* is always situated behind the critical point, at a distance, which is higher for lower frequency and decreases with increasing frequency. Behind this maximum, an interference zone of reflected and head waves is formed and has an oscillatory character.

Other figures in Červený and Hron (1961) show the dependence of plane-wave and spherical-wave reflection coefficients on ratios V_1/V_2 and ρ_1/ρ_2 . Figures for varying ρ_1/ρ_2 show that the largest variations of spherical-wave reflection coefficients can be observed in the critical region. Thus, the critical region is the most favorable region for the determination of densities from the amplitudes of acoustic reflected waves.

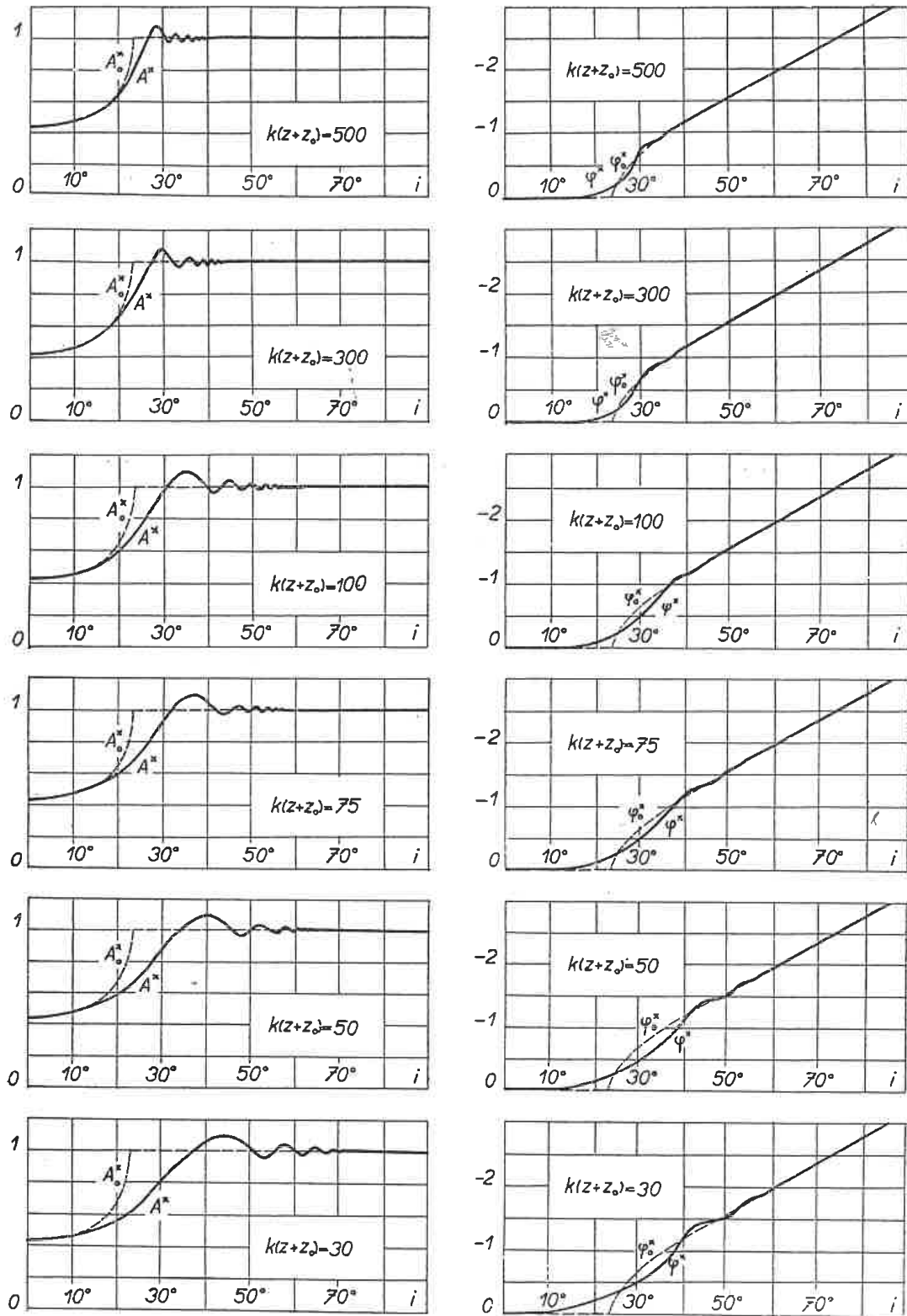


Figure 1: Amplitudes A^* and phases φ^* of spherical-wave reflection coefficients (bold, continuous), and amplitudes A_0^* and phases φ_0^* of plane-wave reflection coefficients (dashed), as a function of the angle of incidence i , for different values of $k(z+z_0)$. Fluid halfspaces with parameters $V_1/V_2 = 0.4$ and $\rho_1/\rho_2 = 1$ are considered. Taken from Červený and Hron (1961). Courtesy Studia geoph. et geod. 5 (1961).

1.2 Elastic case

It is not difficult to generalize the theory and perform the computations also for non-dissipative elastic media. This was done in a number of papers published by V. Červený in 1962-1966. Let us refer here at least to Červený (1965), the most comprehensive of them, giving the detailed derivation, conclusions and results of relevant computations. See also Alulawi and Gurewich (2013).

Whereas the computations of reflection coefficients for spherical acoustic waves using the high-frequency asymptotic methods are highly accurate for any choice of medium parameters, angle of incidence and frequency, the accuracy may decrease for some cases in elastic media, particularly for high-contrast interfaces. Let us consider two elastic media separated by a plane interface, and let us denote their P-wave velocities by α_1 and α_2 , S-wave velocities by β_1 and β_2 , and the mass densities by ρ_1 and ρ_2 . Highest attention was devoted to the practical case of $\alpha_1/\beta_1 \sim \alpha_2/\beta_2 = \sqrt{3}$ and $\rho_1/\rho_2 \sim 1$. In such a case, the reflection coefficients of spherical compressional waves depend primarily on the angle of incidence i , frequency f , and the P-wave velocity contrast α_1/α_2 . For a weak P-wave velocity contrast, i.e. for α_1/α_2 approximately in the interval $0.6 < \alpha_1/\alpha_2 < 0.95$, the asymptotic high-frequency methods give results of a good accuracy. The properties of spherical-wave reflection coefficients of compressional waves are in this case very similar to the properties of acoustic waves, as demonstrated in many figures in Červený (1965). See also a brief discussion in Červený and Ravindra (1971) and Červený, Molotkov and Pšenčík (1977). The accuracy of the spherical-wave reflection coefficients of compressional waves, however, decreases for the interfaces with a high velocity contrast (small α_1/α_2). In this case, it is necessary to compute numerically certain integrals in a complex plane because their analytic computation by asymptotic high-frequency methods is not sufficiently accurate (Červený, 1965).

A big step forward was the invention of the reflectivity method (Fuchs, 1968; Fuchs and Müller, 1971). In the reflectivity method, the reflected waves in a broader sense (including the interference reflected-head wave), reflected at a plane interface between two homogeneous elastic halfspaces, are numerically evaluated by the integration along real-valued axis. The incident wave is generated by a point source situated arbitrarily in one of these halfspaces. The reflected waves are computed in the time domain. The method is highly accurate for any medium parameters and angles of incidence. Using the reflectivity method, we can simply determine reflection coefficients of spherical waves, for incident P as well as S waves. The recent versions of the reflectivity methods can also consider the dissipative media. The dissipative properties of the medium are specified by the P- and S-wave quality factors Q_P and Q_S .

The reflectivity method is preferable and more accurate for the computation of reflection coefficients of spherical waves than the asymptotic high-frequency methods, mainly in the critical and post-critical region. On the other hand, the advantage of the asymptotic method is that it enables to derive certain simple useful analytical relations, which cannot be obtained from the reflectivity method. Let us mention, for example, the approximate relation for the distance between the position of the maximum of the reflection coefficient of a spherical wave and the critical point, and its dependence on frequency f .

In this paper, which has merely a preliminary character, we wish to show how the

reflection coefficients of spherical waves are influenced by the dissipation specified by the quality factor Q . We use the reflectivity method, and the relevant computer program written by Wang (1999).

2 Computation of spherical-wave reflection coefficients for elastic waves by the reflectivity method

We consider two homogeneous elastic non-dissipative halfspaces, which are in a welded contact along a planar interface. We call one of these halfspaces the first halfspace, and the next the second halfspace. The point source of a compressional wave is situated in the first halfspace, at the distance Z_S from the interface. The receiver is also situated in the first halfspace, at a distance Z_R from the interface. The parameters of the first halfspace are denoted by α_1 (velocity of compressional waves), β_1 (velocity of shear waves), ρ_1 (mass density). The parameters of the second halfspace, α_2 , β_2 , and ρ_2 have analogical meaning.

Although in this case we could use the asymptotic high-frequency method with a good accuracy, we use the reflectivity method. The reason is that later we intend to consider the dissipative media, for which the reflectivity method is simply applicable. Using the reflectivity method, we obtain the synthetic seismograms of reflected waves. We obtain the frequency-domain spherical-wave reflection coefficients from the reflectivity time-domain results by applying the Fourier transform. Since we concentrate mostly on study of amplitudes of reflection coefficients, we often use the term “reflection coefficient” to mean its amplitude.

The medium parameters in all computation are as follows:

$$\begin{aligned} \alpha_1 &= 2.0 \text{ km/s} , \quad \beta_1 = 1.156 \text{ km/s} , \quad \rho_1 = 1.0 \text{ km/m}^3 , \\ \alpha_2 &= 2.5 \text{ km/s} , \quad \beta_2 = 1.445 \text{ km/s} , \quad \rho_2 = 1.1 \text{ km/m}^3 , \end{aligned} \quad (2)$$

The distances of the point source and the receiver from the interface are the same, $Z_S = Z_R = 3\text{km}$. Consequently, refraction index $n = \alpha_1/\alpha_2 = 0.8$, the critical angle equals 53.13° , and the critical distance is $r^* = (Z_S + Z_R)\sqrt{1 - n^2}/n = 8 \text{ km}$. The horizontal axes in all following figures represent the offset. In all plots of synthetic seismograms, the vertical axes show the reduced travel time in the form

$$t_{red} = t - \text{offset}/2.5 \quad (\text{second}) . \quad (3)$$

The reduction of travel time decreases considerably the vertical size of plots of theoretical seismograms and makes the shape of individual signals more clear. Unfortunately, the reduction removes the typical hyperbolic form of the complete picture.

In Figure 2, a typical seismogram section of reflected waves (in a generalized meaning, including head waves) generated by the reflectivity program (Wang, 1999) is shown. The critical distance is 8 km. The source-time signal is one period of sinus function, of the duration $\Delta T = 0.1 \text{ s}$. The medium parameters correspond to equation (2). As we can

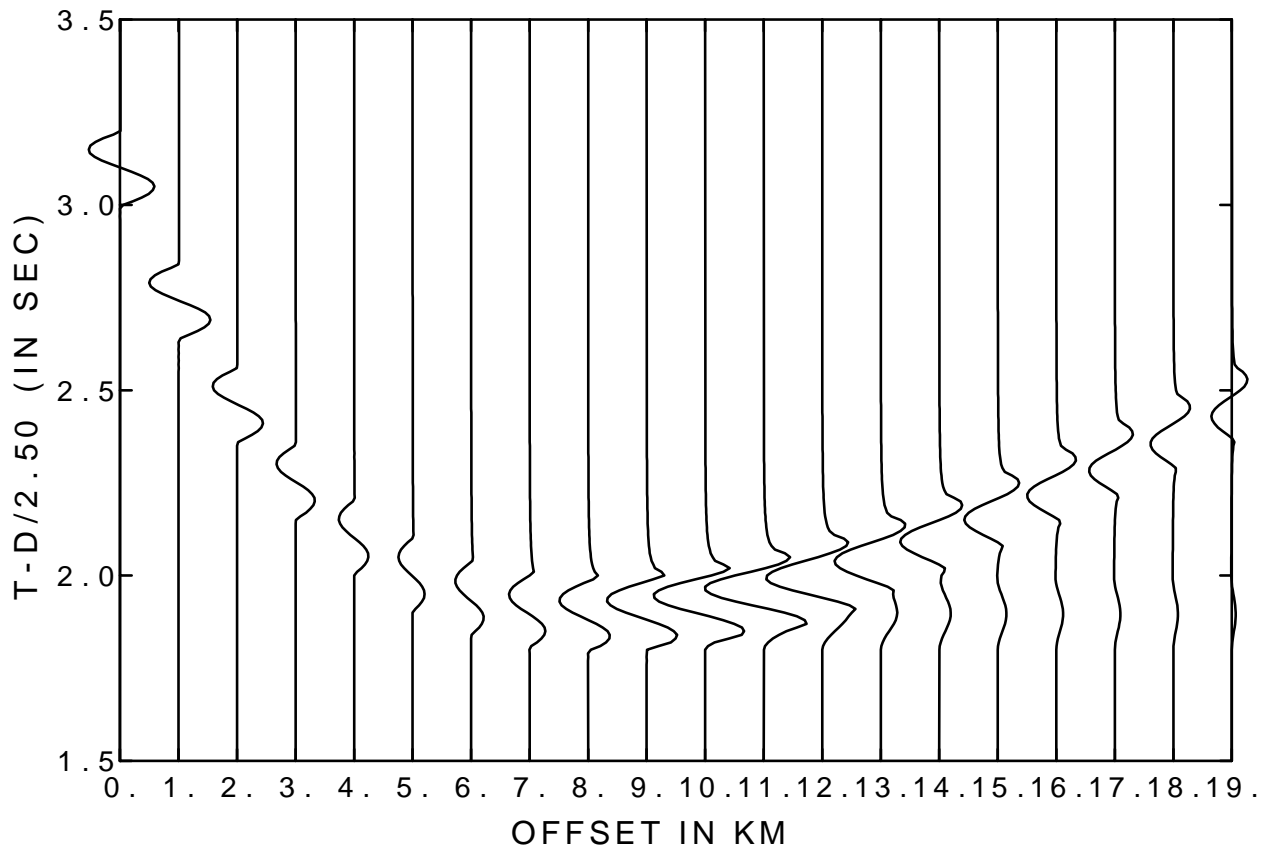


Figure 2: Synthetic seismograms of PP reflected waves generated by a point source. The plane interface between two isotropic perfectly elastic halfspaces, specified by medium parameters (2). The travel time in the vertical axis is reduced. Critical point is situated at 8 km.

see, the behaviour of synthetic seismogram is quite different in the subcritical and overcritical region. In the subcritical region the shape of the signal remains effectively the same as the shape of the source-time signal; only the amplitude of the signal slowly decreases with increasing offset. It has a minimum at the offset of about 5 km, and after it the amplitude signal increases again. Through the critical point, at 8 km, the signal varies smoothly. It has a maximum at about 11 km, and the form of the signal continuously changes. At approximately 13 km, the faster head wave starts to separate from the slower reflected wave. At the offset of separation, the head wave is already very weak, considerably weaker than the reflected wave. Moreover, the amplitude of the head wave decreases very fast with increasing offset, and is hardly visible for largest offsets of 18 km and 19 km. The reflected wave, after the separation from the head wave, is strongly phase shifted. At the last trace, the the shape of the reflected wave corresponds nearly to negative source-time function, as the phase shift is nearly π , for which $e^{-i\pi} \sim -1$.

In Fig. 3, two pictures are presented. The upper picture shows again a synthetic seismogram section of the reflected wave, but for a four time denser system of offsets than in Figure 2. The model parameters and the configuration remain the same as in Figure 2. Also the source-time signal is the same. The bottom plot shows the spherical-wave reflection coefficients, for three frequencies: $f = 10Hz$ (green), $20Hz$ (red) and $30Hz$ (black). These curves of spherical-wave reflection coefficients are computed from the synthetic seismograms shown in the upper plot using the Fourier transform. The spherical-wave reflection coefficients have the same form as the acoustic waves described in the previous section. They are smooth, even in the region around the critical point at 8 km. Behind the critical point, they increase with offset and have a maximum at the offset r_M . The value of r_M is frequency dependent, and increases with decreasing frequency f . Behind the offset r_M , the spherical-wave reflection coefficients oscillate. The oscillations are caused by the interference of reflected and head wave.

The main properties of the coefficients are: 1) The amplitude maxima situated behind the critical point; 2) The oscillatory character of amplitudes in the overcritical region behind the maximum, 3) The position of the maximum behind the critical point frequency dependent. For smaller frequency, the maximum situated at greater distances behind the critical point.

Similar pictures are well known from literature, see, e.g., Červený (1965), Červený and Ravindra (1971), Červený, Molotkov and Pšenčík (1977). In the mentioned references, they were computed mostly by the asymptotic high-frequency method, which yields approximate, but highly accurate, results for the model parameters similar to those given in equation (2). The curves, however, are sometimes presented in different forms. Often, the angle of incidence i is used instead of the offset, similarly as in Figure 1. In some other cases, the amplitudes of vertical or horizontal components of the displacement vector of reflected waves are displayed instead of the amplitudes of the spherical-wave reflection coefficients.

The spherical-wave reflection coefficients in the overcritical region correspond to the superposition of the reflected and head waves. In the synthetic seismograms, the reflected and head waves are fully separated at greater offset behind the critical point, see Figure 2 and the upper plot of of Figure 3. The length of the interference zone of reflected and head waves depends on the form of the source-time signal. Certain important conclusions

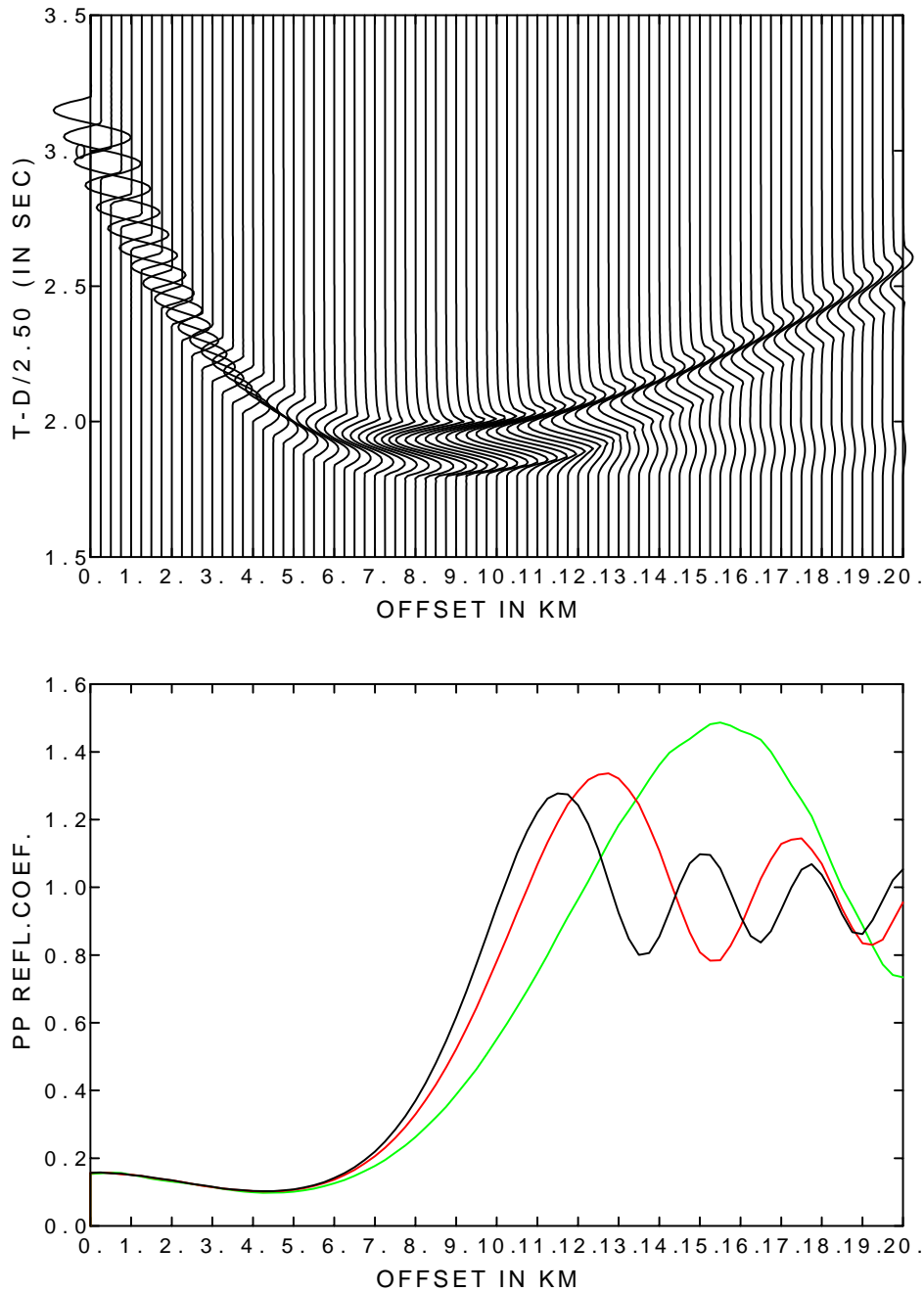


Figure 3: Top: Synthetic seismograms of PP reflected waves generated by a point source, from a plane interface between two isotropic perfectly elastic halfspaces, specified by medium parameters (2). Bottom: Corresponding amplitudes of spherical-wave reflection coefficients for three frequencies: $f = 10\text{ Hz}$ (green), $f = 20\text{ Hz}$ (red), $f = 30\text{ Hz}$ (black). Critical point situated at 8 km.

can be. however, deduced from asymptotic high-frequency investigation, see Červený (1965). They are valid for weak interfaces, with the refraction indices α_1/α_2 not smaller than approximately 0.5:

a) The maximum of the spherical-wave reflection coefficient PP is **always** situated in the interference zone of the reflected and head waves, behind the critical point.

b) At the place where the head wave separates from the reflected waves, the amplitude of the head wave is always considerably smaller than the amplitude of reflected wave.

c) The oscillatory character of the spherical-wave reflection coefficient in the overcritical region is obtained only if both reflected and head waves are considered in Fourier transform, even if they are separated and do not interfere. If, in the region, in which they are separated only the reflected wave is considered, the oscillations vanish.

d) Directly at the critical point the reflected and head waves are singular and their separation has no physical meaning. In the region of the amplitude maximum, however, we can already use well-known asymptotic high-frequency expressions for reflected and head waves, and treat both waves separately. Thus, the spherical-wave reflection coefficient can be calculated by asymptotic high-frequency method already in the vicinity of the maximum of the curve, but both reflected and head waves must be considered.

e) Using the asymptotic high-frequency expressions for reflected and head waves, we can approximately determine the distance between the critical point r^* and the maximum offset r_M of the amplitude of the spherical-wave reflection PP coefficient. It was shown by Červený (1965) that the relation between r_M and r^* is given approximately by the formula

$$r^* = r_M - q(\lambda r_M)^{1/2} , \quad (4)$$

where q is some constant, λ is the wavelength in the first halfspace ($\lambda = \alpha_1/f$).

3 Computation of spherical-wave reflection coefficient of viscoelastic waves by the reflectivity method

Many papers have been devoted to the evaluation of plane-wave reflection coefficients in viscoelastic media. The problem, however, meets difficulties, which are not yet uniquely resolved. We do not discuss these difficulties here; they are well described elsewhere, see, e.g., Krebes and Daley (2007), Sidler, Carcione and Holliger (2008), Daley, Krebes and Lines (2011). Here we devote our attention to the spherical-wave reflection coefficients in viscoelastic media, and use the reflectivity method for their computations. For the use of spherical waves in AVO studies of elastic and anelastic media, see also Haase and Ursenbach (2008).

The older versions of the reflectivity program were written for perfectly elastic media only. Recent versions, however, often consider also dissipative media, specified mostly by the quality factors Q_P and Q_S for P and S waves, respectively. Reflectivity computations in such media do not cause any difficulty, and can be performed for any quality factors. Thus the computation of synthetic seismograms of PP reflected waves, generated by point

sources of compressional waves is straightforward. To get the spherical-wave reflection coefficients from these synthetic seismograms, it is just sufficient to apply the Fourier transform.

In this section, we present several figures, which have the same form as Figure 3. The only difference is that **dissipative media** are considered. The upper plots show synthetic seismograms computed by the version of the reflectivity method, which allows consideration of dissipation (Wang, 1999). The bottom plots show amplitudes of the spherical-wave reflection coefficients for $f = 10, 20$ and 30 Hz, derived from the above seismograms. The parameters α_i, β_i and ρ_i and the configuration remain the same as for Figure 3. The quality factors Q_{P1} and Q_{P2} of P waves in Figures 4-7 are:

$$\begin{aligned}
 \text{Fig.4 : } & Q_{P1} = 10000 , \quad Q_{P2} = 100 , \\
 \text{Fig.5 : } & Q_{P1} = 10000 , \quad Q_{P2} = 50 , \\
 \text{Fig.6 : } & Q_{P1} = 100 , \quad Q_{P2} = 10000 , \\
 \text{Fig.7 : } & Q_{P1} = 100 , \quad Q_{P2} = 100 .
 \end{aligned}
 \tag{5}$$

The values of quality factors of S waves, Q_{S1} and Q_{S2} , are computed from Q_{P1} and Q_{P2} using the approximate formula $Q_{Si} = 2.25Q_{Pi}$, see Müller and Zürn (1984, p. 67).

In a perfectly elastic medium, the quality factor Q_P is infinite. We approximate here the perfectly elastic medium by $Q_P = 10000$. Consequently, we consider the first halfspace in Figures 4 and 5 and the second halfspace in Figure 6 perfectly elastic. In Figure 7, both halfspaces are dissipative.

In synthetic seismograms of reflected waves in Figures 4, 5 and 7, we can see that the head waves are weaker than in Figure 3. This is the effect of dissipation in the second halfspace. The head waves are particularly weak in Figure 5, in which the dissipation is greatest ($Q_{P2} = 50$).

All plots of spherical-wave reflection coefficients are similar to those for a non-dissipative medium shown in Figure 3. In subcritical region, with the exception of a close vicinity of the critical point situated at $r^* = 8\text{km}$, the spherical-wave reflection coefficients for weakly dissipative media are practically independent of frequency. Moreover, they practically do not differ from spherical-wave reflection coefficients for perfectly elastic media.

Directly at the critical point, at 8 km , the spherical-wave reflection coefficients depend on frequency, but only weakly. They also depend on Q_{P1} and Q_{P2} , but again only weakly. It is practically impossible to determine the position of the critical point directly from the measurements of reflected wave seismograms. Even if we determine the position of the critical point indirectly (analytically or using equation (4) from the maximum of the reflection coefficient of spherical waves for a given frequency), it seems improbable that it would be possible to exploit directly the critical point in the solution of inverse problem for quality factors.

At the postcritical offsets, the dominant feature of the spherical-wave reflection coefficient is its maximum at some distance behind the critical point. In practical measure-

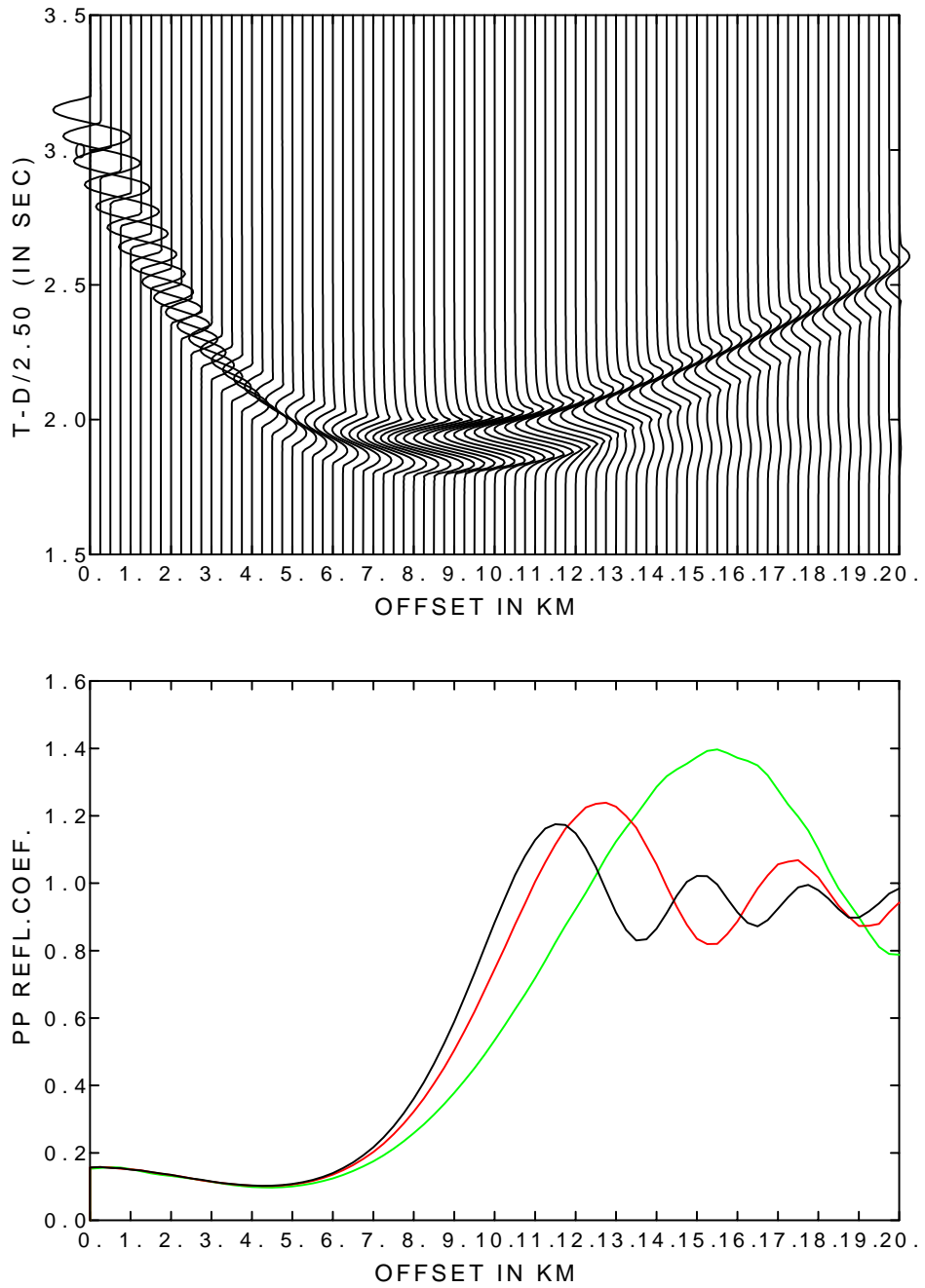


Figure 4: Dtto as in Fig. 3, but for dissipative isotropic media, with $Q_{P1} = 10000$, $Q_{P2} = 100$. Other parameters are the same as in Fig. 3.

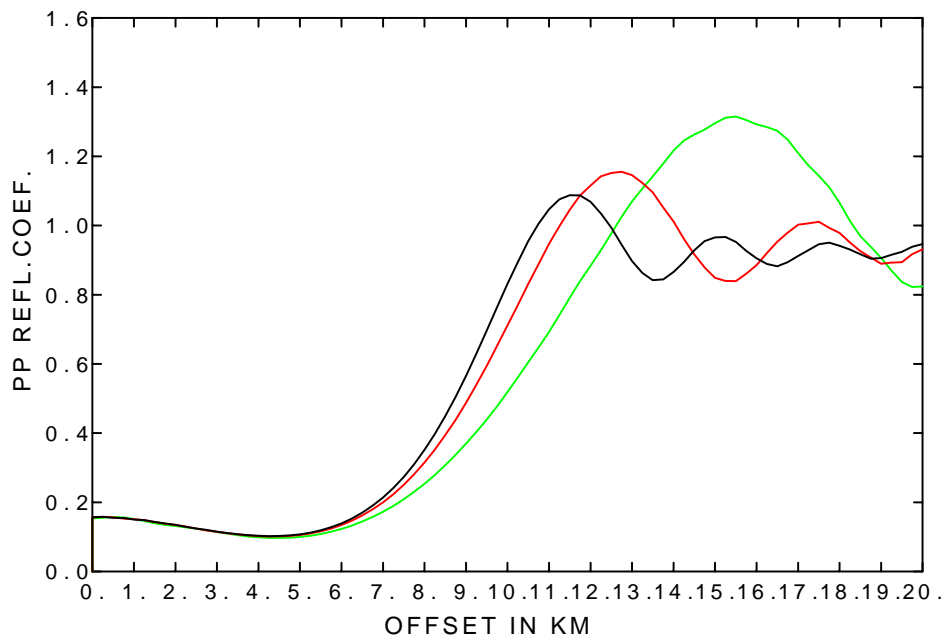
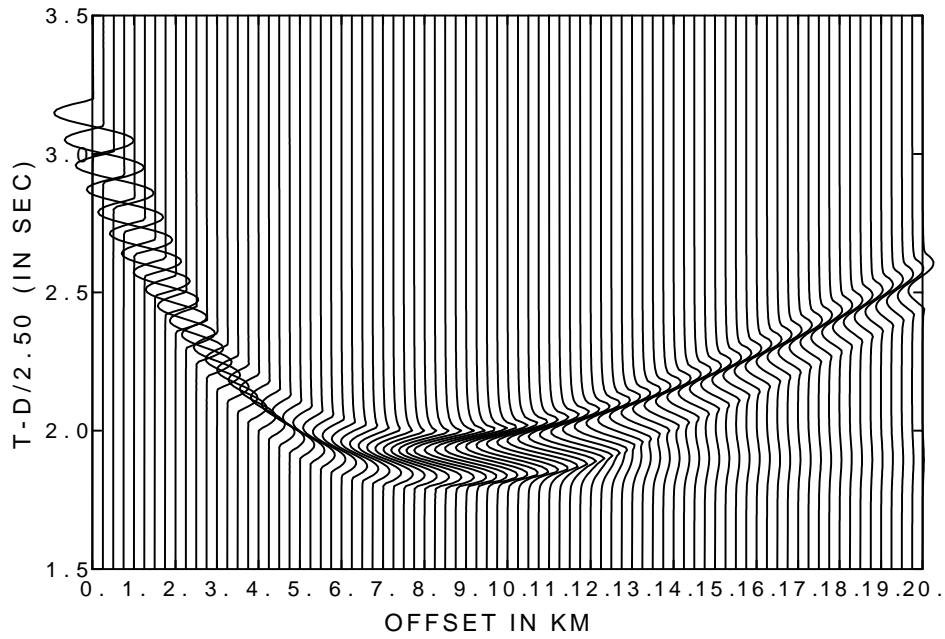


Figure 5: Dtto as in Fig. 3, but for dissipative isotropic media, with $Q_{P1} = 10000$, $Q_{P2} = 50$. Other parameters are the same as in Fig. 3.

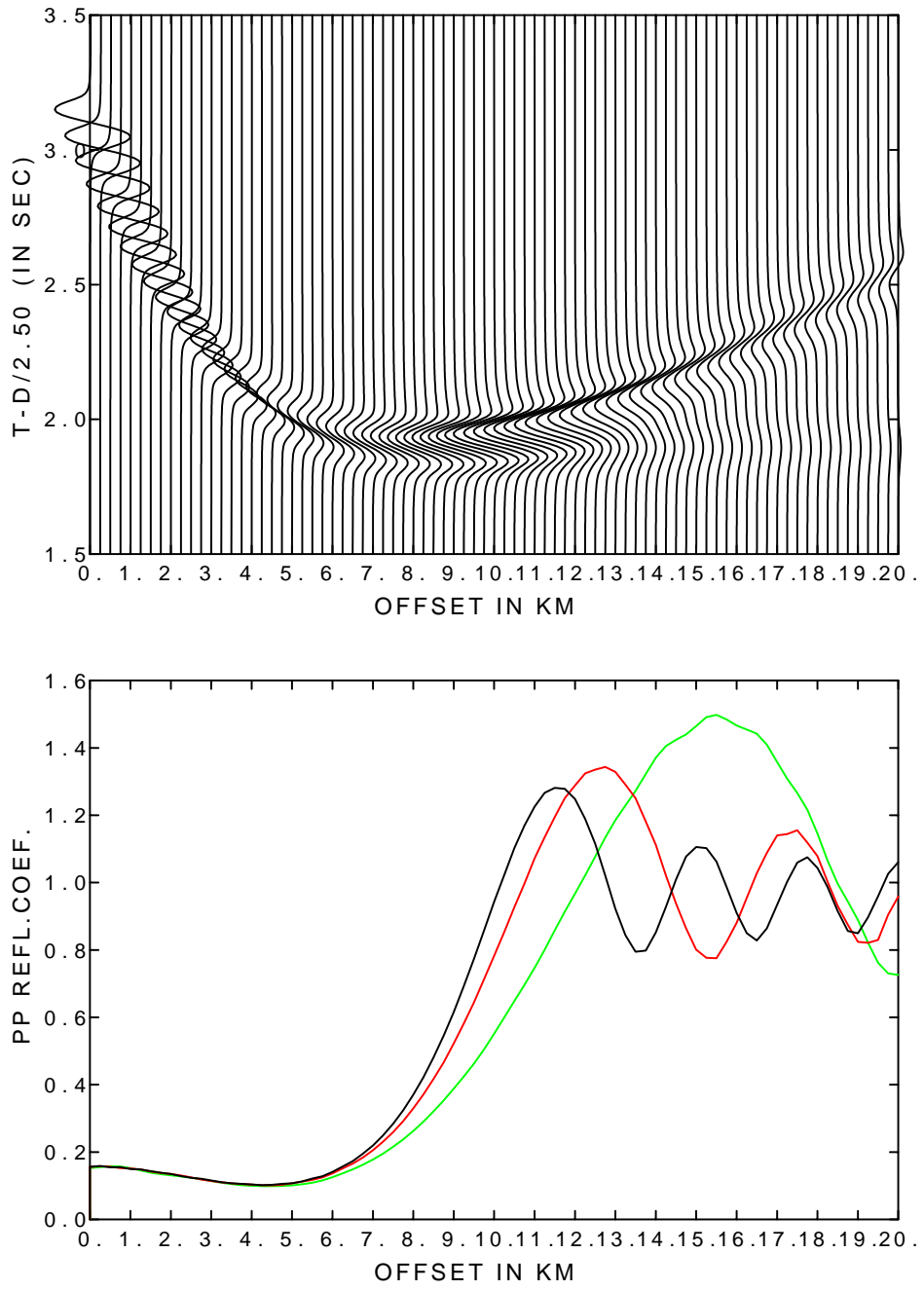


Figure 6: Dtto as in Fig. 3, but for dissipative isotropic media, with $Q_{P1} = 100$, $Q_{P2} = 10000$. Other parameters are the same as in Fig. 3.

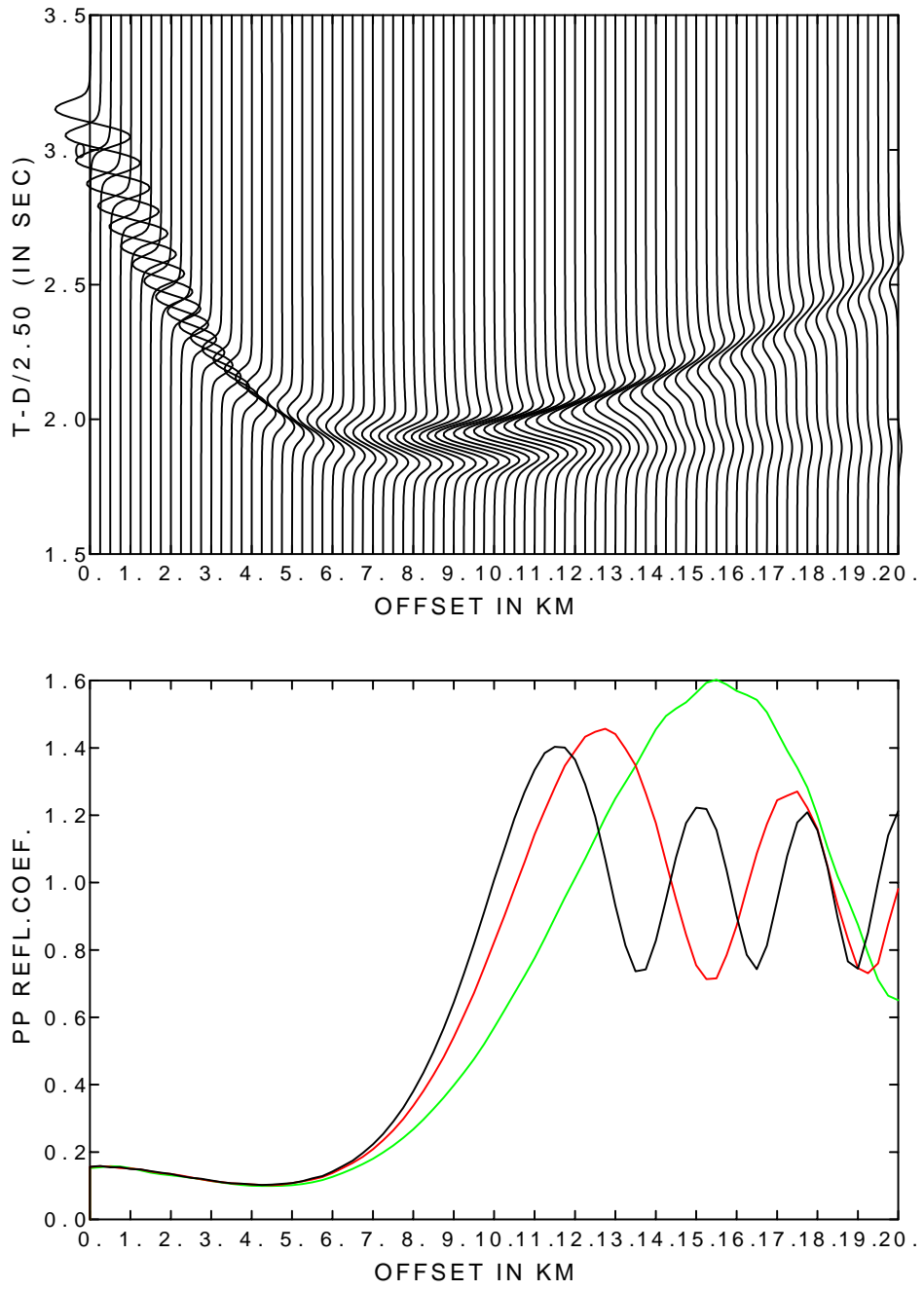


Figure 7: Dtto in Fig. 3, but for dissipative isotropic media, with $Q_{P1} = 100$, $Q_{P2} = 100$. Other parameters are the same as in Fig. 3.

ments, the position of the maximum can be determined simply and with a good accuracy.

The offset $r_M(f)$, at which the maximum of the spherical-wave reflection coefficient is situated for a given frequency f is quite stable. It depends rather strongly on frequency f , but only very weakly on the quality factors Q_{P1} and Q_{P2} . In our case, for frequency $f = 30Hz$, $r_M(f) \sim 11.5$ km, for $f = 20Hz$, $r_M(f) \sim 12.7$ km, and for $f = 30Hz$, $r_M(f) \sim 15.3$ km in all figures, i.e., for perfectly elastic as well dissipative media of varying dissipation. Consequently, the values of Q_{P1} and Q_{P2} do not practically influence the position of the maximum. For weakly dissipative media, this is probably a general property. From the found position of the maximum, we can determine approximately the critical distance r^* , see (4). However, the found position of the maximum cannot be used to determine Q_{P1} and Q_{P2} .

The quantity which really depends on Q_{P1} and Q_{P2} is not the position of the maximum for a given frequency, but the value of the amplitude of the spherical-wave reflection coefficient for a given frequency. We must, however, relate this value to some other measurable quantity. If it is possible to determine the maximum and the following minimum of the amplitude of the coefficient, then the differential offset $D(f)$ between the maximum and the following minimum is the sought quantity, which depends on Q_{P1} and Q_{P2} for a given frequency. Figures 3-7 confirm this clearly.

In this study, we concentrated on the amplitudes of the spherical-wave reflection coefficients and we did not study the phases of the spherical-wave reflection coefficients for dissipative media although they are obtained automatically, if the Fourier transform of reflected wave seismograms is performed. The advantage of the phase-distance curves is that they are smoother and the oscillations are milder than of the amplitude-distance curves, see Figure 1 for acoustic waves in non-dissipative media. For perfectly elastic media, the phase curves have been used for inversion of data by Zhu and McMechan (2013), where the advantages of phase versus offset (PVO) are also explained. We believe that it would be possible to use them in a similar way for weakly dissipative media.

Acknowledgements

The research has been supported by the Grant Agency of the Czech Republic under the contracts P210/11/0117 and P210/10/0736, by the Ministry of Education of the Czech Republic within Research Project MSM0021620800 and by the Consortium Project "Seismic Waves in Complex 3-D Structures".

References

- Alulawi, B., and Gurevich, B., 2013. Analytic wavefront curvature correction to plane-wave reflection coefficient for a weak contrast interface. *Geophysical Prospecting*, **61**, 53–63.
- Brekhovskikh, L.M., 1957. *Waves in Layered Media* (in Russian). Akad. Nauk SSSR, Moscow. Translated to English in 1960 by Academic Press, New York.
- Červený, V., 1965. The dynamic properties of reflected and head waves around the critical point. *Geofyzikální sborník 1965*, 135–245.
- Červený, V., and Hron, F., 1961. Reflection coefficients for spherical waves. *Studia geoph. et geod.*, **5**, 122–132.
- Červený, V., Molotkov, I.A., and Pšenčík, I., 1977. *Ray method in seismology*. Universita Karlova, Praha.
- Červený, V., and Ravindra, R., 1971. *Theory of seismic head waves*. Univ. of Toronto Press, Toronto.
- Daley, P.F., Krebes, E.S., and Lines, L.R., 2011. Reflected PP arrivals in anelastic media. *J. Seis. Exploration*, **20**, 57–72.
- Haase, A.B., and Ursenbach, C.P., 2008. Spherical wave AVO modeling in elastic and anelastic two-layer media. *J. Seis. Exploration*, **17**, 85–208.
- Krebes, E.S., and Daley, P.F., 2007. Difficulties with computing anelastic plane-wave reflection and transmission coefficients. *Geophys. J. Int.*, **170**, 205–216.
- Müller, G., and Zürn, W., 1984. Seismic waves and free oscillations. In: *Landoldt-Börnstein: Numerical Data and Functional Relationships in Science and Technology, Vol. 2: Geophysics of the Solid Earth, the Moon and the Planets*, pp. 61–70. Springer Verlag, Berlin.
- Sidler, R., Carcione, J.M., and Holliger, K., 2008. On the evaluation of plane wave reflection coefficients in anelastic media. *Geophys. J. Int.*, **175**, 94–102.
- Skopintseva, L., Ayzenberg, M. Landr o, M., Nefedkina, T.V., and Aizenberg, A.M., 2011. Long-offset AVO inversion of PP reflections from plane interfaces using effective reflection coefficients. *Geophysics*, **76**, C65–C79.
- Wang, R., 1999. A simple orthonormalization method for stable and efficient computation of Green's functions. *Bull. Seismol. Soc. Am.*, **89**, 733–741.
- Xinfa Zhu, and McMechan, G.A., 2012. Elastic inversion of near- and postcritical reflections using phase variations with angle. *Geophysics*, **77**, R149–R159.